NREL
NATIONAL RENEWABLE ENERGY LABORATORY

Evaluating Solar Resource Data Obtained from Multiple Radiometers Deployed at the National Renewable Energy Laboratory

Preprint

A. Habte, M. Sengupta, and A. Andreas
National Renewable Energy Laboratory

S. Wilcox and T. Stoffel
Solar Resource Solutions

To be presented at the European Photovoltaic Solar Energy Conference and Exhibition
Amsterdam, Netherlands
September 22–26, 2014

NREL is a national laboratory of the U.S. Department of Energy
Office of Energy Efficiency & Renewable Energy
Operated by the Alliance for Sustainable Energy, LLC

This report is available at no cost from the National Renewable Energy Laboratory (NREL) at www.nrel.gov/publications.

Conference Paper
NREL/CP-5D00-62775
Revised December 2015

Contract No. DE-AC36-08GO28308

NOTICE

This report is available at no cost from the National Renewable Energy Laboratory (NREL) at www.nrel.gov/publications.

Available electronically at http://www.osti.gov/scitech

Available for a processing fee to U.S. Department of Energy and its contractors, in paper, from:

U.S. Department of Energy
Office of Scientific and Technical Information
P.O. Box 62
Oak Ridge, TN 37831-0062
phone: 865.576.8401
fax: 865.576.5728
email: mailto:reports@adonis.osti.gov

Available for sale to the public, in paper, from:

U.S. Department of Commerce
National Technical Information Service
5285 Port Royal Road
Springfield, VA 22161
phone: 800.553.6847
fax: 703.605.6900
email: orders@ntis.fedworld.gov
online ordering: http://www.ntis.gov/help/ordermethods.aspx

Cover Photos: (left to right) photo by Pat Corkery, NREL 16416, photo from SunEdison, NREL 17423, photo by Pat Corkery, NREL 16560, photo by Dennis Schroeder, NREL 17613, photo by Dean Armstrong, NREL 17436, photo by Pat Corkery, NREL 17721.

Errata

Figure 5 was revised in December 2015 to correct an error in the calculation to derive the values. The error does not affect any other parts of the publication.

EVALUATING SOLAR RESOURCE DATA OBTAINED FROM MULTIPLE RADIOMETERS DEPLOYED AT THE NATIONAL RENEWABLE ENERGY LABORATORY

Aron Habte
Manajit Sengupta
Afshin Andreas
National Renewable Energy Laboratory
15013 Denver West Parkway, Golden, CO 80401, USA
aron.habte@nrel.gov
manajit.sengupta@nrel.gov
afshin.andreas@nrel.gov

Stephen Wilcox
Solar Resource Solutions, LLC
swilcox303@gmail.com

Thomas Stoffel
Solar Resource Solutions, LLC
tstoffelSRS@gmail.com

ABSTRACT: Solar radiation resource measurements from radiometers are used to predict and evaluate the performance of photovoltaic and concentrating solar power systems, validate satellite-based models for estimating solar resources, and advance research in solar forecasting and climate change. This study analyzes the performance of various commercially available radiometers used for measuring global horizontal irradiances (GHI) and direct normal irradiances (DNI). These include pyranometers, pyrheliometers, rotating shadowband irradiometers, and a pyranometer with a shading ring deployed at the National Renewable Energy Laboratory's Solar Radiation Research Laboratory (SRRL). The radiometers in this study were deployed for one year (from April 1, 2011, through March 31, 2012) and compared to measurements from radiometers with the lowest values of estimated measurement uncertainties for producing reference GHI and DNI. The differences among radiometer measurements were calculated using the mean bias error and root mean square error methods, in which the GHI and DNI values from individual instruments were compared to concurrently computed GHI reference and measured reference DNI. The differences were calculated as a percent of reading for solar zenith angles ranging from 17.5 degrees to 85 degrees (the range of available solar zenith angles throughout the year at SRRL, excluding data near sunrise and sunset). Under clear-sky conditions when the solar zenith angle was less than 60 degrees, differences of less than 5% were observed for both GHI and DNI measurements when they were compared to the reference radiometers. These normalized differences increased during partly cloudy sky conditions and when the solar zenith angle was greater than 60 degrees. The intent of this paper is to present a general overview of each radiometer's performance. The National Renewable Energy Laboratory made no effort to ensure that the radiometers presented here were representative units; therefore, this paper does not guarantee the same results for all radiometers from the same manufacturer or model.
Keywords: Global Horizontal Irradiance; GHI; Direct Normal Irradiance; DNI; Diffuse Horizontal Irradiance; DHI; Pyranometer; Pyrheliometer; Rotating Shadowband Irradiometer; Solar Radiation Measurements

1 INTRODUCTION

Accurate measurements of solar resources are essential for the successful deployment and reduction of investment risks in photovoltaic and concentrating solar power systems [1]. Solar resources could be obtained from ground-based monitoring station and/or satellite-based models. They are complementary: the former provides the accuracy and shorter time data interval necessary for many renewable energy technologies; the latter provides broader spatial coverage. In this paper, we focus on the ground-based solar resource measurements from radiometers. The National Renewable Energy Laboratory's (NREL's) Solar Radiation Research Laboratory (SRRL) collects and disseminates ground-based solar resource data through the Measurement and Instrumentation Data Center.[1] The center provides historical solar data from multiple radiometers with calibration traceability to the Système International d'Unités through the World Radiometric Reference [2]. This paper provides a comprehensive estimation of differences associated with radiometric data obtained from various radiometers under all sky conditions with respect to a reference determined to provide the lowest estimated uncertainties. Some of the variables contributing to the differences include radiometer calibrations and each instrument's response characteristics to variations in solar zenith angle, spectral irradiance distributions, temperature, installation (e.g., tilt), aging, nonlinearity, and incomplete knowledge of environmental conditions. The solar measurements from the radiometers were quality assessed to minimize erroneous data; however, these data are presented with some caveats: (1) An ample number of radiometers for each model was not available to provide representative sample data for each manufacturer's product. (2) In our professional experience, we have found that each instrument responds differently under various climatic/weather conditions; thus, these results are limited to the conditions encountered at SRRL in Golden, Colorado, USA (39.742° N, 105.18º W, 1,829 m AMSL) during the period of analysis. (3) Solar irradiance on the Earth's surface is extremely variable, and these instruments have variable time responses, spectral components, cosine responses, and temperature sensitivities; thus, the limited data set and specific location used for this study are not intended to be used by the reader to infer any general conclusions of radiometer performance beyond the context of our evaluations. This paper intends to provide the reader with a general understanding about how each radiometer behaves under specific documented conditions compared to the selected reference data.

[1] http://www.nrel.gov/midc

2 METHOD

Data from 32 global horizontal irradiance (GHI) and 19 direct normal irradiance (DNI) radiometers are presented in this paper (See Table 1 and Table 2). The performance of each instrument was derived from time-series measurements relative to the corresponding reference irradiance. Reference data were obtained using a Kipp and Zonen CH1 (DNI) instrument and an Eppley Laboratory, Inc., black-and-white model 8-48 (diffuse horizontal irradiance, or DHI) instrument. Additionally, the reference GHI were calculated from a component sum method using measurements from the CH1 and 8-48 radiometers (Equation 1). The resulting performance analyses for the 1-minute and hourly data set are based on the mean bias error (MBE) and root mean square error (RMSE) methods.

The reference radiometers were calibrated with absolute cavity radiometers traceable to the World Radiometric Reference using NREL's Broadband Outdoor Radiometer Calibration process[2] [3]. This method provides the lowest calibration and measurement uncertainties for both GHI and DNI irradiances [4][5][6]. Further, various data quality schemes were applied to the radiometric data to remove any erroneous measurements and ensure that the data were suitable for comparative analyses. Specifically, a data quality assessment software tool (SERI_QC) was applied to each data point. The relationship of broadband solar radiation components is shown in Equation 1.

$$\boldsymbol{GHI = DNI * Cos\,(Solar\ Zenith\ Angle) + DHI} \quad (1)$$

SERI_QC is based on a normalization process involving dimensionless parameters including clearness or cloudiness index (Kt), effective diffuse horizontal transmittance (Kd), and direct beam transmittance (Kn) derived from the corresponding extraterrestrial radiation [7].

Table 1: GHI Instrument List

Inst. #	Instrument Type	Model	Ratio	Manufacturer and Comment	Inst. #	Instrument Type	Model	Ratio	Manufacturer
1	Thermopile	CM22[a]	1.01	Kipp & Zonen - Ventilated	17	Semiconductor	RSR2 (secondary)	0.99	Irradiance, Inc./ LI-COR - Experimental instrument; not for sale
2	Thermopile	CM6b[a]	1.01	Kipp & Zonen	18	Thermopile	TSR-590	0.96	YES, Inc.
3	Thermopile	CM3-CNR1[a]	1.01	Kipp & Zonen - Does not have a relatively clear view of the sky (current)	19	Thermopile	TSR-591	0.95	YES, Inc.
4	Thermopile	PSP[a]	1.00	Eppley Laboratory, Inc. - Ventilated, thermal, and zenith corrected	20	Thermopile	TSR-592	0.96	YES, Inc.
5	Thermopile	PSP[a]	1.00	Eppley Laboratory, Inc. - Thermal and zenith corrected	21	Thermopile	TSR-590-LH[b]	0.97	YES, Inc. - Correction applied
6	Thermopile	PSP[a]	0.99	Eppley Laboratory, Inc. - Ventilated	22	Thermopile	TSR-591-LH[b]	0.97	YES, Inc. - Correction applied
7	Thermopile	PSP[a]	1.00	Eppley Laboratory, Inc.	23	Thermopile	TSR-592-LH[b]	0.97	YES, Inc. - Correction applied
8	Thermopile	TSP-700[a]	1.01	YES, Inc. - Ventilated	24	Thermopile	TSR-590-JM[c]	0.99	YES, Inc. - Correction applied
9	Thermopile	TSP-1[a]	1.00	YES, Inc. - Ventilated	25	Thermopile	TSR-591-JM[c]	0.99	YES, Inc. - Correction applied
10	Thermopile	SPN1[a]	1.03	Delta-T	26	Thermopile	TSR-592-JM[c]	0.98	YES, Inc. - Correction applied
11	Semiconductor	SPLite[a]	1.01	Kipp & Zonen	27	Thermopile	SR11-7196	0.97	Hukseflux
12	Semiconductor	SP-110[a]	1.06	Apogee	28	Thermopile	SR11-7242	0.98	Hukseflux
13	Semiconductor	LI-200[a]	1.01	LI-COR	29	Thermopile	LP02-41120	0.99	Hukseflux
14	Semiconductor	P007	1.00	David Brooks - Experimental sensor	30	Thermopile	LP02-41272	0.97	Hukseflux
15	Semiconductor	ATI	1.00	Ascension Technology, Inc., RSR /LI-COR	31	Semiconductor	NREL-CRADA-RSR2	0.98	Irradiance Inc./LI-COR
16	Semiconductor	RSR2	0.98	Solar-Mil.-CRADA-RSR/ LI-COR	32	Semiconductor	Solar-Mil.-CRADA-RSR	1.00	Solar Millennium AG./Reichert Gmbh/LI-COR[b] - Not available (Solar Millennium, Inc., is out of business)

[a] Current NREL calibration factor used during the period of the evaluation
[b] Lee Harrison
[c] Joseph Michalsky

[2] http://www.nrel.gov/aim/borcal.html

Table 2: DNI Instrument List

Inst. #	Instrument Type	Model	Ratio	Manufacturer/Comment
1	Thermopile	NIP2[a]	0.99	Eppley Laboratory, Inc.
2	Thermopile	NIP1[a]	0.99	Eppley Laboratory, Inc.
3	Semiconductor	LI-201[a]	0.94	LI-COR[b] - Experimental instrument; not for sale
4	Semiconductor	ATI/ LI-COR	1.04	Ascension Technology Inc./LI-COR[b]
5	Semiconductor	RSR/ LI-COR	0.98	Irradiance Inc./LI-COR[b] - Experimental instrument; not for sale
6	Thermopile	TSR-590	0.99	YES, Inc.[b]
7	Thermopile	TSR-591	0.97	YES, Inc.[b]
8	Thermopile	TSR-592	0.99	YES, Inc.[b]
9	Thermopile	TSR-590LH	0.99	YES, Inc.[b]
10	Thermopile	TSR-591LH	0.98	YES, Inc.[b]
11	Thermopile	TSR-592LH	0.99	YES, Inc.[b]
12	Thermopile	TSR-590JM	0.98	YES, Inc.[b]
13	Thermopile	TSR-591JM	0.97	YES, Inc.[b]
14	Thermopile	TSR-592JM	0.97	YES, Inc.[b]
15	Semiconductor	NREL-CRADA-RSR2/LI-COR	0.98	Irradiance Inc./LI-COR[b]
16	Thermopile	SPN1[a]	1.05	Delta-T[b]
17	Thermopile	DR018066	0.97	Hukseflux
18	Thermopile	DR018068	0.98	Hukseflux
19	Semiconductor	Solar-Mil.-CRADA-RSR/ LI-COR	1.00	Solar Millennium AG./Reichert Gmbh/LI-COR[b] - Not available (Solar Millennium, Inc., is out of business)

[a] Current NREL calibration factor used during the period of the evaluation
[b] Calculated using global and diffuse measurements

To remove potential instrument calibration biases, the radiometric data from the test instruments were normalized to the reference data. Normalizing the data to a common reference allowed us to compare the environmental effects of each instrument's performance, which was the stated focus of this study. Normalization was carried out by isolating all the irradiance data for the study period (April 1, 2011, through March 31, 2012) between 44- and 46-degree solar zenith angles and summing all the data in this solar zenith angle range for each radiometer. The specified solar zenith angle range was selected to conform to the NREL convention of reporting all broadband radiometer calibrations at a 45-degree solar zenith angle. A ratio was then obtained by dividing each test radiometer summation by the sum of the reference data for the same conditions. The ratio for each test radiometer was then used to acquire the new normalized irradiance value by dividing each test irradiance value for the time interval by the normalization ratio.

Further, concurrent data from a Yankee Environmental Systems, Inc., total sky imager (TSI) model TSI-880 were used to categorize irradiance data from all the instruments according to clear-, partly cloudy, and mostly cloudy sky conditions. The data from the TSI-880 helped us better understand the irradiance differences among the instruments relative to sky conditions (Figure 1).

3 RESULTS AND DISCUSSION

Both GHI and DNI test instruments were evaluated using a reference DNI and a reference DHI following the component sum method (Equation 1). The figures discussed in the results section show the performance of each test instrument relative to the reference instrument under various sky conditions.

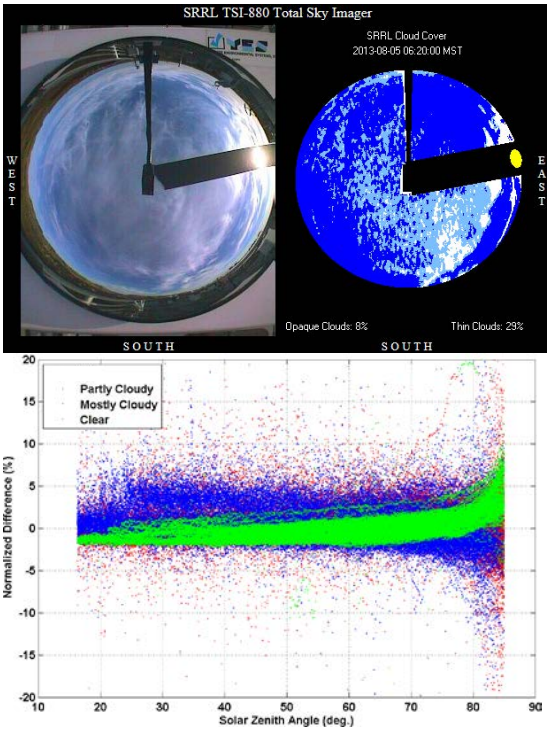

Figure 1: Example plots showing how the TSI-880 sky imager is used to partition the sky condition: (top) instantaneous image and (bottom) results for all the data of one instrument.

3.1 GHI Comparisons

Comparisons of the hourly average GHI data for all 32 instruments under test are shown in Figure 2. The MBE and RMSE in percent are shown for each instrument number. The yellow box illustrates 95% confidence interval coverage, and the red line is the mean point for the 95 % confidence interval area. These plots demonstrate the relative tendencies or performance of each instrument with respect to the references used in the study. The figures also illustrate the skewness of the differences when the MBE percent tended to the positive on some of the instruments and negative on others. These characteristic differences were used to identify the overestimation or underestimation of irradiance by each test instrument. Under clear-sky conditions, the relative differences appeared to exhibit less bias, and the mean differences (red line) for most test instruments tended to have less variability than they did under the mostly cloudy sky conditions. In addition, test instruments that showed higher variability above the confidence interval box, either positive or negative trends, tended to have relatively poorer performance in the higher zenith angles. Further, both the MBE and RMSE values should be taken into consideration to understand the performance of each instrument relative to the reference instrument. For example, one instrument could have less bias but higher RMSE; therefore, an instrument with less bias and less RMSE would perform similarly to the reference data. However, the higher RMSE in the partly and mostly cloudy sky conditions could be largely attributed to changing sky conditions and associated with differing time responsivity of the radiometers [8].These conditions also apply to the DNI data set comparison.

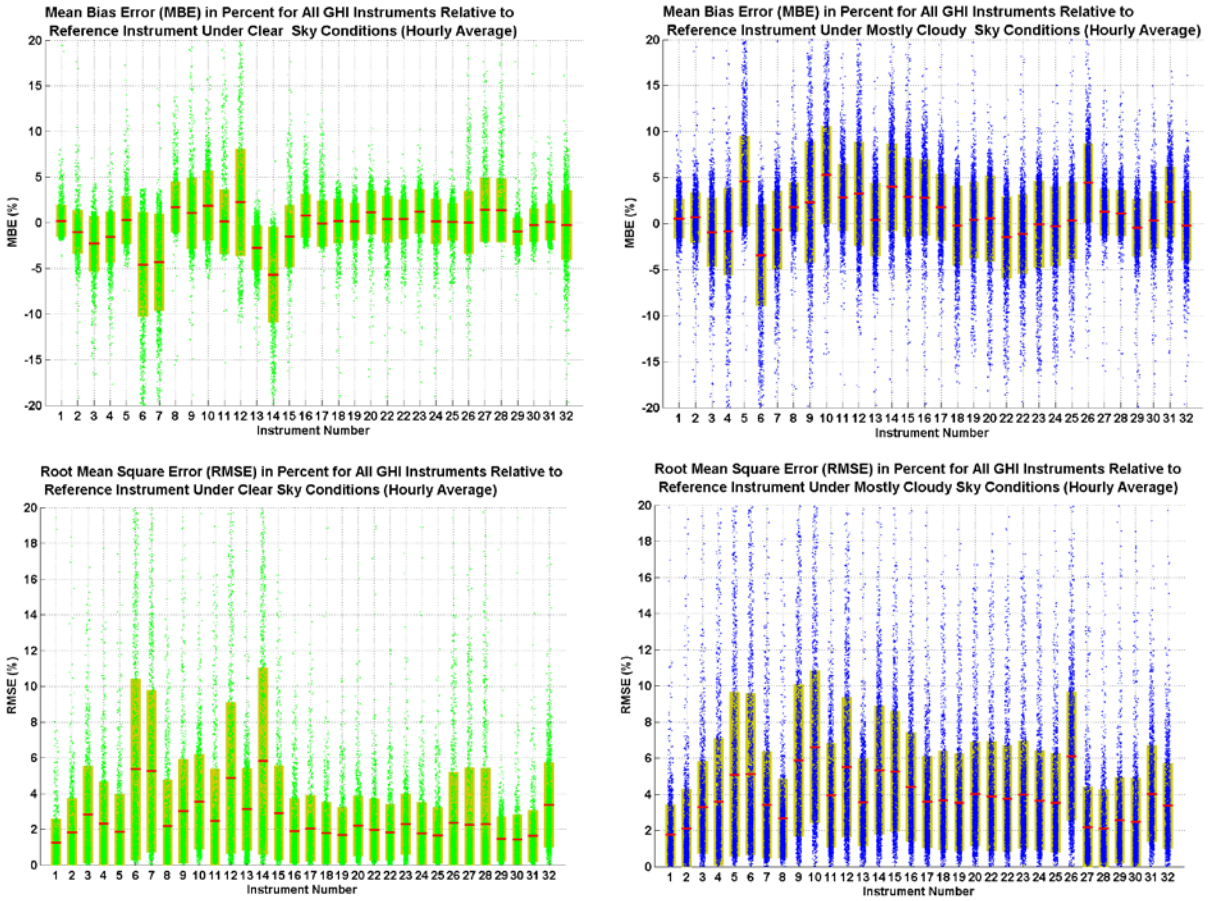

Figure 2: Clear- and mostly cloudy sky conditions: (top) MBE and (bottom) RMSE in percent for the hourly average for all GHI data under study. The red line signifies the mean value of the differences for the 95% confidence level.

The study also analyzed the performance of silicon photodiodes. For instance, LI-COR (LI-200), which are fast-responding sensors, sample a smaller portion of the solar spectrum (400 nm to 1,100 nm), but they are calibrated to a thermopile output range (300 nm to 4,000 nm). These silicon instruments tend to have reasonable accuracy under the calibration conditions, but they have spectral, angular, and temperature sensitivity issues that contribute to significant differences under conditions other than the calibration conditions [9][10][11]. The RSR2 instrument has a built-in correction algorithm in the data acquisition system supplied by the manufacturer.[3] These algorithms apply different correction methods to minimize the above-mentioned issues. It appears that the application of such algorithms in the RSR2 minimized the deviation of the data relative to the reference instrument. The RSR2 uses a LI-COR LI-200 sensor, and Figure 3 demonstrates the comparison results between the RSR2 and LI-200 sensors for GHI irradiance relative to the reference instrument data. The LI-200 instrument does not have spectral, angular, or temperature sensitivity corrections. Between the two instruments, a clear shift of the probability distribution for the clear-sky condition from negative errors for the LI-200 to less and relatively normally distributed errors for the RSR2 was observed. However, in the mostly cloudy sky condition, the probability distribution errors shifted more to the positive MBE for the RSR2.

[3] http://www.irradiance.com/

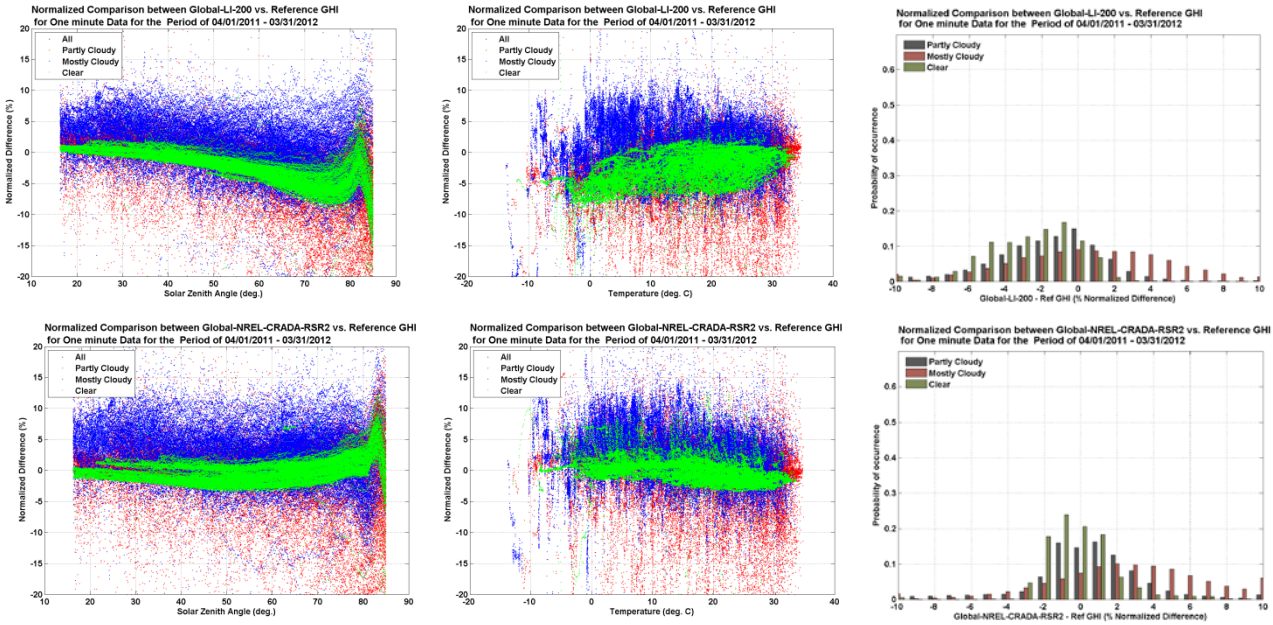

Figure 3: (Top) Comparison of the uncorrected silicon photodiode sensor to the (bottom) corrected silicon photodiode—RSR2. Note: Green dots represent clear-, red dots represent partly cloudy, and blue dots represent mostly cloudy sky conditions.

Further, the temperature dependence of thermopile instruments, such as the Eppley precision spectral pyranometer (PSP), was analyzed. The thermopile radiometers equilibrate to ambient temperature, which is typically higher than the sky temperature, and this creates an infrared energy imbalance between the thermopile radiometer and the sky. This situation produces a thermal energy exchange in which the thermopile emits energy to the sky [4], and this was evident in the data as a negative output of irradiance by the thermopile radiometers in the absence of solar radiation. For this reason, some of the thermopile radiometers have an infrared correction to offset this thermal imbalance applied in the data using coincident measurements from a pyrgeometer. The ventilated Eppley PSP radiometer in this study is equipped with ventilators.

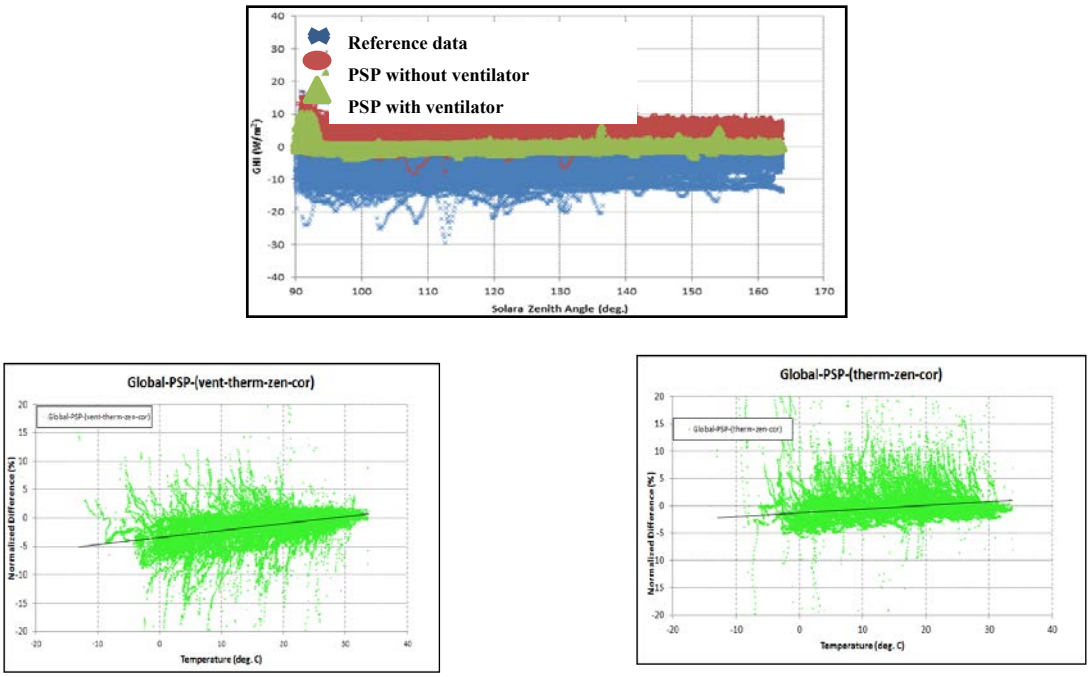

Figure 4: Understanding nighttime thermal offset (top) under all sky conditions and (bottom) normalized differences (UUT minus reference) versus temperature for (left) ventilated and (right) unventilated Eppley Laboratory, Inc., PSP radiometers under clear-sky conditions (1-minute data)

The purpose of the ventilators is to remove any accumulation of dust, snow, frost, dew, etc., from the dome of the radiometers and to discourage the presence of insects. Although both the Eppley ventilated and unventilated radiometers were corrected for thermal offset, the ventilator on the ventilated PSP tended to affect the irradiance by creating an additional temperature imbalance between the case and dome of the instrument. This scenario was more apparent during cold ambient temperatures (as shown in the bottom left plot of Figure 4). Usually during overcast skies, the ambient and sky temperatures are near equilibrium; however, the ventilator was generating additional heat to the radiometer, which we postulated, creating an additional exchange of energy between the radiometer and the sky. This situation ultimately increased the negative bias within the radiometer. Further, this condition could be exacerbated if the ventilator filter of the PSP is uncleaned for some time and airflow is restricted. The ventilator effect appeared to be particularly noticeable during nighttime (as shown in the top plot of Figure 4). However, a couple of important observations are worth mentioning here. The thermal offset correction for the ventilated PSP was performed using a ventilated Eppley precision infrared radiometer (PIR), but if the flow of the air that is caused by the ventilators in both the precision infrared radiometer and the PSP is not equivalent—for example, because of a difference in the amount of dirt or other obstruction in the PSP and PIR—then the results as shown in the bottom left plot of Figure 4 could be justified.

On the other hand, we used a ventilated PIR to correct the unventilated PSP (as shown in bottom right plot of Figure 4). This correction method stipulates that similar ventilation systems be used to correct both the precision infrared radiometer and the PSP, and this could be the reason for an overestimation of irradiance for the unventilated Eppley PSP.

3.1 DNI Comparisons

Nineteen DNI data sets were included in the DNI analysis. Some of the instruments had a calculated DNI value, and others had a direct measurement of DNI. Some test radiometers, such as the silicon photodiode instruments from rotating shadowband irradiometers, have a calculated DNI. These instruments measure GHI and DHI irradiance components. The resulting DNI is then computed using Equation 1. However, [9] describes how the computed DNI from these instruments produce an approximate 7% error because these instruments are susceptible to spectral sensitivity and the spectral distributions of GHI and DHI at the time of measurement. These errors in GHI and DHI propagate to the DNI calculations, thereby resulting in larger errors in the calculated DNI.

The analysis suggests that the smaller differences were demonstrated among the instruments under clear-sky conditions than other sky conditions. The two Eppley Laboratory Inc., normal incidence pyrheliometers (NIP) and the two Hukseflux model "DR" types had smaller MBE than others under clear-sky conditions (as shown in the top left of Figure 5).

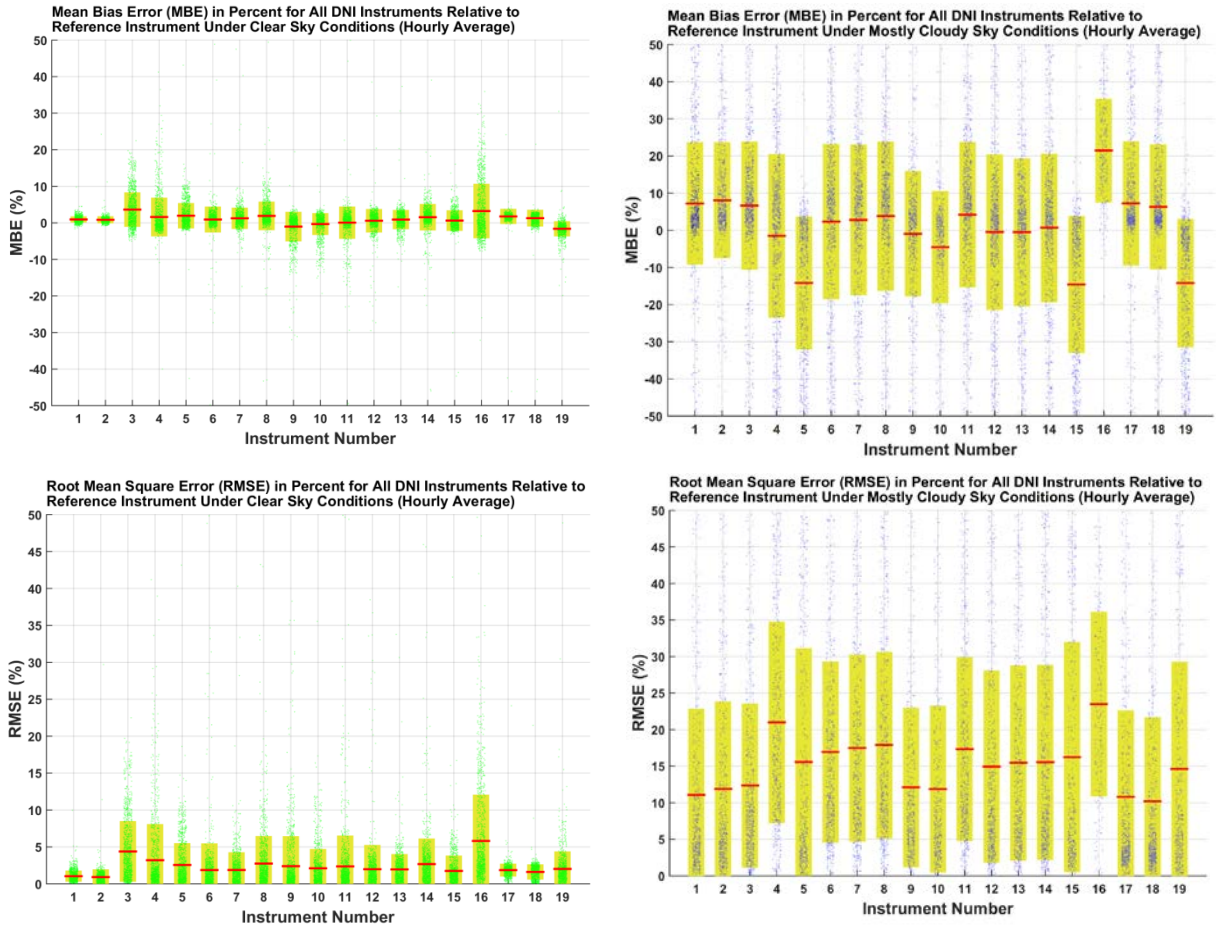

Figure 5: Clear- and mostly cloudy sky conditions: (top) MBE and (bottom) RMSE in percent for the hourly average for all DNI data under study. The red line signifies the mean value of the differences for the 95% confidence level.

However, the DNI results suggest more variable performance than the GHI comparisons under variable sky conditions (Figure 5). These larger deviations could have been a result of fast-moving clouds and differing radiometer response times accompanied by differing fields of view [8]. The reader should further note that much of the data in the mostly cloudy conditions have small irradiance levels, and the ratio among the small numbers can present unrealistically alarming ratios in which the actual differences in solar irradiances is quite small.

The DNI instruments also have temperature dependence. For instance, the Hukseflux radiometer model number DR108068 had relatively more evident temperature dependence than model number DR108066 (Figure 6). The two Eppley NIP radiometers tended to have less temperature dependences, especially at temperatures below 20°C. The two NIPs did not have temperature corrections, and the two Hukseflux radiometers did not have the temperature corrections either; however, a previous study that included the Hukseflux radiometers showed that the manufacturers' temperature corrections curve for these instruments reduced temperature error to a much lower magnitude. Correction for temperature dependence for pyrheliometers assists in acquiring less overall uncertainty [5].

4 SUMMARY AND CONCLUSION

Accurate solar resource measurements are essential for understanding solar energy conversion system performance, developing improved satellite-based models for estimating solar resources at the Earth's surface, validating solar radiation forecasts, and advancing climate science. The measured irradiance data for this study were normalized to radiometer angular responsivities corresponding to a 45-degree solar zenith angle. This caused a difference of approximately 2% on average for both GHI and DNI between normalized values and those from the instrument's calibration factor. Under clear-sky conditions when the solar zenith angle was less than 60 degrees, differences of less than 5% were observed for both GHI and DNI measurements when compared to the reference radiometers. For data during periods when the solar zenith angle was greater than 60 degrees, differences in GHI under mostly cloudy and clear-sky conditions increased to 17%. Differences of up to 40% in DNI measurements on a few instruments were found for high solar zenith angles under mostly cloudy sky conditions. Some of these differences were expected from the various instrument design characteristics for time response, spectral response, cosine response, and temperature response; however, the differences were higher for silicon photodiode instruments with no spectral, cosine, and/or temperature correction.

It must be noted that the estimated measurement uncertainties of the reference radiometers and the data logger system were *not* included in our results; therefore, the interpretation of the MBE and RSME differences observed for the normalized data in this study must exceed the estimated expanded uncertainties of the reference and test instruments to be statistically significant. However, relative differences among instruments provide a valid and useful comparison.

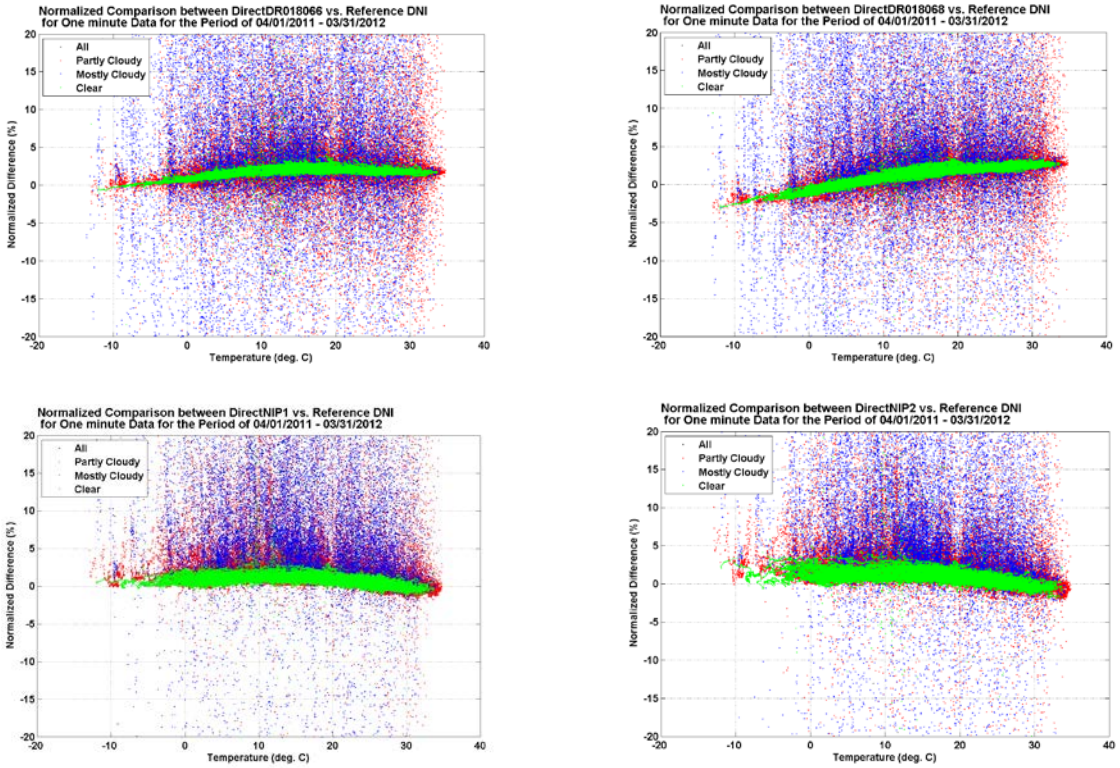

Figure 6: Effect of temperature on DNI measurement
Note: Green dots represent clear, red dots represent partly cloudy, and blue dots represent mostly cloudy sky conditions

5 ACKNOWLEDGEMENT

This works was supported by the U.S. Department of Energy under Contract No. DE-AC36-08GO28308 with the National Renewable Energy Laboratory.

6 REFERENCES

[1] Stoffel, T.; Renne, D.; Myers, D., Wilcox, S.; Sengupta, M.; George, R.; Turchi, C. (2010). Concentrating Solar Power: Best Practices Handbook for the Collection and Use of Solar Resource Data (CSP). NREL/TP-550-47465. Golden, CO: National Renewable Energy Laboratory.

[2] Stoffel, T.; Reda, I. (2013). National Renewable Energy Laboratory Pyrheliometer Comparisons: 24 September–5 October 2012 (NPC-2012). NREL/TP-5500-58430. Golden, CO: National Renewable Energy Laboratory.

[3] Myers, D.R.; Andreas, A.; Stoffel, T.; Reda, I.; Wilcox, S.; Gotseff, P.; Kay, B. (2001). "Radiometric Calibrations, Measurements, and Standards Development at NREL." NCPV Program Review Meeting Proceedings; Oct. 14–17, Lakewood, Colorado. NREL/CP-560-30964. Golden, CO: National Renewable Energy Laboratory.

[4] Myers, D.R. (2013). Solar Radiation: Practical Modeling for Renewable Energy Applications. Boca Raton, FL: CRC Press, Taylor and Francis Group.

[5] Michalsky, J.J., et al. (2011). "An Extensive Comparison of Commercial Pyrheliometers Under a Wide Range of Routine Observing Conditions." Journal of Atmospheric and Oceanic Technology (28); pp. 752–766.

[6] Habte, A.; Wilcox, S.; Stoffel, T. (2014). Evaluation of Radiometers Deployed at the National Renewable Energy Laboratory's Solar Radiation Research Laboratory. 187 pp.; NREL/TP-5D00-60896. Golden, CO: National Renewable Energy Laboratory.

[7] Maxwell, E.; Wilcox, S.; Rymes, M. (1993). User's Manual for SERI_QC Software: Assessing the Quality of Solar Radiation Data. NREL/TP-463-5608. Golden, CO: National Renewable Energy Laboratory.

[8] Vignola, F.; Stoffel, T.; Michalsky, J.J. (2012). Solar and Infrared Radiation Measurements. Boca Raton, FL: CRC Press, Taylor and Francis Group.

[9] Myers, D.R. (2011). "Quantitative Analysis of Spectral Impacts on Silicon Photodiode Radiometers." American Solar Energy Society Solar Conference Proceedings; May 17–20, Raleigh, North Carolina. Boulder, CO: American Solar Energy Society.

[10] Vignola, F. "Removing Systematic Errors From Rotating Shadowband Pyranometer Data." (2006). American Solar Energy Society Solar Conference Proceedings; July 9–13, Denver, Colorado. Boulder, CO: American Solar Energy Society.

[11] King, D.L.; Myers, D.R. (1997). "Silicon-Photodiode Pyranometers: Operational Characteristics, Historical Experiences, and New Calibration Procedures." 26th Institute of Electrical and Electronics Engineers Photovoltaic Specialists Conference Proceedings; Sept. 29–Oct. 3, Anaheim, California.